XIV National School on Superconductivity, Ostrów Wielkopolski, October 13–17, 2009

Manganites — Structural Aspects

A. Szytuła

M. Smoluchowski Institute of Physics, Jagiellonian University, Reymonta 4, 30-059 Kraków, Poland

In memory of Professor Jan Stankowski

In the work a brief discussion of the structural and magnetic properties of the manganites from the point of view of the micro- and macrostructures is presented. The influence of stoichiometry with the different oxygen parameter δ and doped atoms is discussed. The correlation between the crystal structure parameters and magnetic properties for some manganites is presented.

PACS numbers: 61.05.cp, 61.05.F−, 61.05.J−, 75.30.kz, 75.50.Ee, 75.50.−y

1. Introduction

Manganese perovskites with the general formula $A_{1-x}A'MnO_{3+\delta}$ (A = La, rare earth, A′ = rare earth, Ca, Sr, Ba, etc.) were discovered in the 1950's [1] and soon after their properties were extensively studied. The interest in the manganite has been renewed in connection with the discovery of colossal magnetoresistance (CMR) [2, 3]. Structural and magnetic properties of these compounds are sensitive both to the manganese valence and to internal (chemical) factors.

The family of these compounds, where the formula can be written in a general way as ABO_3, is the mineral "perovskite" ($CaTiO_3$) form of the ideal cubic structure (space group $Pm\bar{3}m$). In the crystal unit cell the atoms occupy the following positions: A (0, 0, 0), B (1/2, 1/2, 1/2) and O (1/2, 0, 1/2), (1/2, 1/2, 0) and (0, 1/2, 1/2). The stability of this structure is governed by the structural factor $t = \frac{r_A + r_O}{\sqrt{2}(r_B + r_O)}$, where r_A, r_B, and r_O are the radius of A^{3+}, B^{3+} and O^{2-} ions. For t between 0.8 and 1.0 the above mentioned type of crystal structure is stable. With changes in the valence of the ions the ionic radius changes and this could lead to a structural phase transition to the rhombohedral or orthorhombic phase and changes in the magnetic properties. The magnetic properties are correlated with the short and/or long-range charge, orbital and spin order. Significant role plays here also the separation of the phases with different properties and the Jahn–Teller effect which causes a distortion of the lattice. The role of these factors is discussed in the paper [4].

In this work the different points concerning the structural aspects and their influence on the magnetic properties of these compounds will be successively reviewed below.

2. Results

2.1. Influence of stoichiometry

$LaMnO_3$ has the orthorhombic crystal structure (space group $Pnma$) and is antiferromagnetic with the Néel temperature equal to 140 K. Their magnetic structure is represented by an antiferromagnetic lattice consisting of ferromagnetic layers of Mn magnetic moments but the alternating (100) planes have the opposite spin directions. The Mn^{3+}–O^{2-}–Mn^{3+} ions are coupled ferromagnetically in the (001) planes and antiferromagnetically along the c-axis [5]. The exchange integrals are equal to +0.83 and −0.58 meV, respectively [6]. The influence of the nonstoichiometry on the magnetic properties is observed in $LaMnO_{3+\delta}$ systems. The increase of δ up to 0.1 does not cause any change in the crystal structure but changes the magnetic properties: the coexistence of the antiferro- and ferromagnetic ordering for $\delta = 0.025$ and 0.07 and ferromagnetic ordering for $\delta = 0.1$ is observed. For $\delta = 0.15$ the change of the crystal structure to a hexagonal one is observed (see Table I).

TABLE I

Structural and magnetic data for $LaMnO_{3+\delta}$ compounds. δ — the oxygen parameter, σ_{JT} — the Jahn–Teller distortion parameter, $T_{N,C}$ — the Néel or Curie temperature, μ_{AF} — magnetic moments in the antiferro- and μ_F — in the ferromagnetic phase [7].

δ	0	0.025	0.07	0.1	0.15
Mn^{4+} [%]	0	5	14	20	30
at 1 K	O ($Pnma$)	O	O	O	H(R-3c)
cryst. structure					
at 300 K	O	O	O	H	H
1 K	0.106	0.065	0.023	0.003	0
$\sigma_{JT} \times 10^2$ [Å]					
(300 K)	0.15	0.18	0.008	0	0
Type of magn. ord.	AF	F+AF	F+AF	F	F
$T_{N,C}$ [K]	140	110	160	150	160
μ_{AF} [μ_B]	3.49	2.52	0.25		
μ_F [μ_B]		1.48	3.25	2.86	0.78

The change of the magnetic properties is accompanied by a drastic reduction of the static Jahn–Teller distortion of the MnO_6 octahedra. The magnetic behaviour is interpreted by taking into account two effects caused by the increase in δ: the cation vacancies and the Mn^{4+}/Mn^{3+} ratio enhancement. The increase in the ferromagnetic interaction up to $\delta = 0.07$ can be explained by the increase in both the Mn^{4+} ions concentration and the Mn–O–Mn

bond angle value, which favor the Mn^{4+}–O^{2-}–Mn^{3+} double exchange interaction. For $0.025 \leq \delta \leq 0.07$ the phase separation is also observed [7].

The deficit of the La or Mn atoms leads also to the change of magnetic properties from antiferro- to a ferromagnetic [8–10].

2.2. Influence of doped atoms

For the mixed manganites with the chemical composition $R_{1-x}A_xMnO_3$, where R is a trivalent rare earth ion (La^{3+}, Pr^{3+}, Nd^{3+}) and A is replaced by a divalent ion (Sr^{2+}, Ca^{2+}, Ba^{2+}) the phase diagrams indicate the change of the magnetic structure and transport properties in a function of the A^{2+} ion content from an antiferromagnetic insulator for $x = 0$ to a ferromagnetic metallic for $x > 0$. The magnetic phase boundary separates also a low temperature metallic phase from a high-temperature insulating one. It results in very large values of magnetoresistance at T_c [3, 11].

The explanation of these complex properties gives the electron diffraction experiment carried out for $La_{0.5}Ca_{0.5}MnO_3$. This compound is an antiferromagnet below $T_N = 155$ K and a ferromagnetic between T_N and $T_C = 225$ K. In the electron diffraction pattern at $T = 95$ K the additional reflection described by the propagation vector $\boldsymbol{k} = (1/3, 0, 0)$ or $(0, 1/3, 0)$ is observed. This ordering exists up to T_C. The electron microscopy confirms the existence of stripes with the period of 11 Å for $x = 0.5$ and 16.5 Å for $x = 0.67$ [12]. The existence of the stripes is connected with the charge-ordering as well as with the order of d_{z^2} orbital of the Mn^{3+} ions. In the $Pr_{1-x}Ca_xMnO_3$ ($x = 0.4$ and 0.5) compound a correlation between charge, orbital and spin ordering is observed [13]. Analysis of the diffraction pattern obtained by the synchrotron radiation indicates existence of three groups of the Bragg reflections:

— $(0, 2k, 0)$, where k is an integer number corresponding to the fundamental reflection,

— $(0, 2k + 1, 0)$ is connected with the charge order,

— $(0, k + 1/2, 0)$ is connected with the orbital order.

The intensities of the Bragg reflections connected with the charge and the orbital order decrease to zero at $T_0 = 245$ K, whereas the antiferromagnetic order disappears at $T_N \approx 175$ K.

The analysis of the half-width at the half-height of the Bragg reflections gives the correlation length of the orbital order equal to 320(10) Å for $x = 0.4$ and 160(10) Å for $x = 0.5$ while the orbital order correlation length is larger than 2000 Å [13].

Neutron diffraction data give the following values of the magnetic correlation lengths: 200–400 Å for Mn^{3+} ion and > 2000 Å for Mn^{4+} ions. This result suggests the correlation between the magnetic and the orbital or the charge order.

Very interesting results were obtained by the investigations of the isotopic effect. In the $(La_{1-y}Pr_y)_{0.7}Ca_{0.3}MnO_3$ compounds substitution of the ^{16}O isotope by ^{18}O caused the change of the transport properties from metal to insulator [14]. For compounds with $y = 0.75$ neutron diffraction data for the sample with the ^{18}O isotope give an additional reflection of the magnetic origin correlated with the propagation vector $\boldsymbol{k} = (1/2, 0, 1/2)$ which corresponds to an antiferromagnetic structure. These data indicate a noncollinear structure for the ^{16}O and a collinear one for the ^{18}O isotope compounds. The magnetic phase diagrams determined for $(La_{1-y}Pr_y)_{0.7}Ca_{0.3}MnO_3$ have similar character for both isotopes. For large concentration of the Pr atoms an antiferromagnetic and an insulator (AF–I) phase is observed. With decreasing Pr content firstly the coexistence of the AF–I and ferro-metallic (FM) phase is observed and then, for small concentration of Pr, only FM phase exists. The value of critical Pr concentration y that leads to this phase change is equal to:

isotope ^{16}O:	0.45,	0.56,
isotope ^{18}O:	0.6,	0.84.

Different properties are observed in $La_{1-x}R_xMnO_{3+\delta}$ (R = Pr, Nd) with $\delta \approx 0.07$ which corresponds to the 14% concentration of Mn^{4+}. In these compounds La and R ions are trivalent. The compounds crystallize in an orthorhombic crystal structure (space group *Pnma*). The composition dependence of the lattice parameters a, b, and c for both systems is similar. Replacement of the La^{3+} ions with the ionic radius (1.061 Å) by smaller Pr^{3+}(1.160 Å) or Nd^{3+}(0.995 Å) ions causes a decrease in these parameters (Fig. 1).

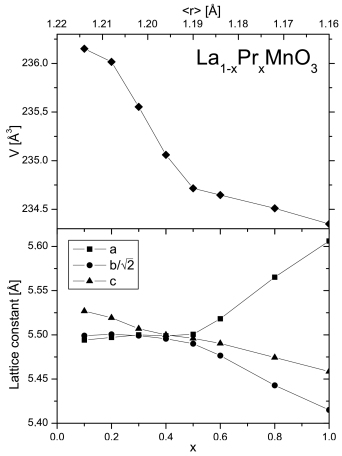

Fig. 1. Dependence of the lattice parameters (a, $b/\sqrt{2}$ and c) and the unit cell volume (V) on the Pr content in $La_{1-x}Pr_xMnO_3$ determined basing on the X-ray diffraction data collected at room temperature in the function of x and the average ions radius in the A sublattice $\langle r_A \rangle$ [17].

TABLE II

Calculated values of the coherent Jahn–Teller distortions determined using the relation (1) and the orthorhombic lattice distortion D for $La_{1-x}Nd_xMnO_3$ [18].

x	0	0.1	0.3	0.3	0.4	0.5	0.6	0.7	0.8	0.9	1.0
D [%]	1.84	2.076	2.256	2.524	2.61	2.66	2.74	2.84	3.54	3.645	3.748
$\sigma_{JT} \times 10^2$ [Å]	1.1	1.1	1.1	1.8	2.0	2.6	3.4	5.6	6.4	7.8	7.18

For $x \leq 0.4$ the lattice parameters a, $b/\sqrt{2}$, and c are nearly equal which indicates a pseudocubic phase O* [15]. With increasing x a strong anisotropy of these parameters is observed. For the large x value the orthorhombic phase O′ is observed. In this region the lattice parameters obey the relation $b/\sqrt{2} \leq c \leq a$. This dependence implies the isotropic Mn–O and Mn–Mn distances for $x \leq 0.4$ and strong anisotropy of these values for $x > 0.4$. These suggest that the distortion of the MnO_6 octahedra caused by the cooperative Jahn–Teller effect increases with increasing x while the Mn–O–Mn angle (φ) decreases linearly. The values of φ are significantly different from 180° implicating a strong distortion of the crystal structure. The distortion site is connected with the Jahn–Teller effect. The Jahn–Teller distortions were determined using the relation

$$\sigma_{JT} = \sqrt{\left[(\text{Mn}-\text{O})_i - \langle \text{Mn}-\text{O} \rangle\right]^2 / 3}\,, \qquad (1)$$

where $(\text{Mn–O})_i$ are the experimental values of the interatomic distances determined from the X-ray and neutron diffraction experiments and $\langle$Mn–O$\rangle$ is the average bond length. The value of the σ_{JT} parameter increases with increasing x (see Table II). This is in good agreement with the change of the temperature distortion T_{JT}. Figure 2 shows the concentration x dependence of the critical temperature of the magnetic origin and T_{JT} temperature of the orbital order–disorder transition. In $LaMnO_3$ at $T_{JT} = 780$ K a distortion of the MnO_6 octahedra and an orbital ordering is observed. In the $La_{1-x}Nd_xMnO_6$ systems the values of T_{JT} linearly increase with increasing Nd content up to 1175 K [16]. The values of T_{JT} are correlated with the orthorhombic lattice distortion $D = \sum[a_i - a]/3a$, where $a = (ab/\sqrt{2}c)^{1/3}$ and $a_1 = a$, $a_2 = b/\sqrt{2}$ and $a_3 = c$. The critical temperature of the magnetic ordering decreases slowly up to $x = 0.6$ for R = Pr and $x = 0.4$ for R = Nd. For higher values of x the decrease of the critical temperature of the magnetic ordering is quick. This change accompanies the decrease in the unit cell volume V and Mn–O–Mn bond angle and a strong anisotropy of the Mn–Mn and Mn–O distance in the a–c plane and along the b-axis. The decrease in the $T_{C,N}$ values is connected with the increase in the Jahn–Teller distortion and increase of the doped atoms concentration.

Magnetic and neutron diffraction data show complex magnetic properties. The Bragg peaks in the neutron diffraction pattern correspond for $x \leq 0.6$ ferro- while

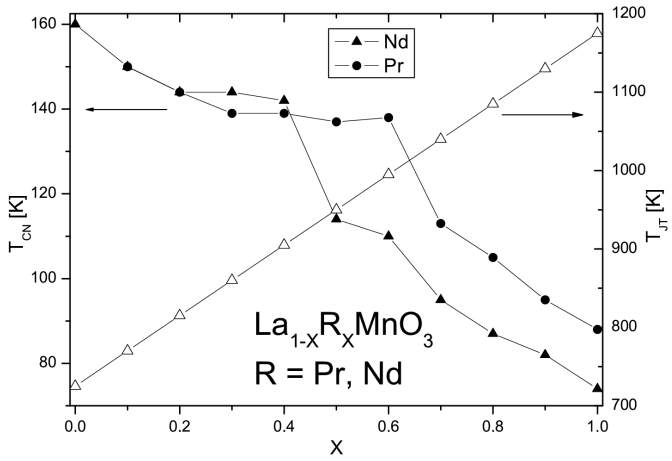

Fig. 2. Concentration dependence of the critical temperatures of the Mn magnetic moment for $La_{1-x}R_xMnO_3$ (R = Pr, Nd) [17, 18] and T_{JT} temperature of the orbital order–disorder transition for $La_{1-x}Nd_xMnO_3$ [16].

for $0.7 \leq x \leq 0.9$ correspond to ferro- and antiferromagnetic structures. This suggests the coexistence of two phases with different magnetic ordering or canted magnetic structure. The presented result does not give a clear distinction between those possibilities. The doped Pr^{3+} or Nd^{3+} ions cause also a decrease in the critical temperature of the magnetic phase transitions. In $RMnO_3$ (R = Pr and Nd) the Mn magnetic moments form a collinear structure [17, 18]. In $NdMnO_3$ the Nd magnetic moments order ferromagnetically at low temperatures which are in good agreement with the temperature dependence of the ac magnetic susceptibility and the specific heat measurements [19].

The value of the Mn magnetic moment in the ferromagnetic phase is close to 3.5 μ_B which confirms that, in the sample, there is a mixture of the Mn^{3+} ions with the electronic structure $(t_{2g}^3 e_g^1)$ and the magnetic moment equal to 4 μ_B and Mn^{4+} with t_{2g}^3 and $\mu = 3$ μ_B. The ratio of Mn^{4+}/Mn^{3+} does not change with changes in the concentration x.

3. Summary

The results presented in the paper show strong correlation between the crystal structure parameters and

magnetic properties of the manganites. The non-stoichiometry and doped atoms cause the changes in the magnetic properties as a result of introduced holes in the Mn sites. The properties of the manganites are sensitive to "chemical factors" (the valence of the ions). For example, the $LaMnO_3$ compound contains Mn^{3+} ions which are the Jahn–Teller ions. If a fraction x of the trivalent La^{3+} ions are replaced by the divalent Sr^{2+}, Ca^{2+} or Ba^{2+} ions, holes are introduced on the Mn sites. This results in a fraction $1-x$ of the Mn ions remaining as Mn^{3+} $(3d^4, t_{2g}^3 e_g^1)$ and a fraction x becoming Mn^{4+} $(3d^3, t_{2g}^3 e_g^0)$. In the Mn^{3+} ion, the t_{2g} electrons are tightly bound to the ion but e_g electron is itinerant. The hopping of the e_g electrons between the Mn sites induces the double exchange interaction [20]. There are two possible interactions between orbitals of the Mn ions:

(i) superexchange t_{2g}(Mn)–$2p_\pi$(O)–t_{2g}(Mn),

(ii) double exchange e_g(Mn)–$2p_\sigma$(O)–e_g(Mn).

The competition between these two interactions leads to the different types of magnetic ordering and complex magnetic phase diagrams observed in the mixed manganites. The majority of these compounds crystallize in the orthorhombic crystal structure. In this structure the Jahn–Teller effect is observed and influences the crystal structure and magnetic properties. In some manganites it is connected with the charge order or separation of different phases connected with the spin order (antiferro- and ferromagnetic) in the microscopic scale over many tens of nanometers. In the case of thin films a charge order at the centers of domain walls is observed. This promotes charge ordering on short length scales [4]. In the complex oxides and manganites ordered or disordered structures are observed over different length scales. The differences in ionic radius generate long-range effects leading to new structural symmetries. Long-range correlations can also lead to metallic behaviour, ferromagnetism and charge-ordered stripes.

Acknowledgments

The author thanks Dr. Teresa Jaworska–Gołąb, Dr. Bogusław Penc and Mrs. Krystyna Grzelak for help in preparation of the manuscript of this paper.

References

[1] G.H. Jonker, J.H. van Santen, *Physica* **16**, 337 (1950).

[2] R. von Helmolt, J. Wecker, B. Holzapfel, L. Schultz, K. Samwer, *Phys. Rev. Lett.* **71**, 2331 (1993).

[3] S. Jin, T.H. Tiefel, M. McCormack, R.A. Fastnacht, R. Ramesh, J.H. Chen, *Science* **264**, 413 (1994).

[4] N. Mathur, *Nature* **400**, 405 (1999).

[5] E.O. Wollan, W.C. Koehler, *Phys. Rev.* **160**, 545 (1955).

[6] F. Moussa, M. Henion, J. Rodriguez-Carvajal, M. Moudden, L. Pinsard, P. Revcolevschi, *Phys. Rev. B* **54**, 15149 (1996).

[7] C. Ritter, M.R. Ibarra, J.M. De Teresa, P.A. Algarabel, C. Marquina, J. Blasco, J. Garcia, S. Oseroff, S.W. Cheong, *Phys. Rev. B* **56**, 8902 (1997).

[8] A. Arulraj, R. Mahesh, G.N. Subbana, R. Mahendiran, A.K. Raychandhuri, C.N.R. Rao, *J. Solid, State Chem.* **127**, 87 (1996).

[9] R. Dhahri, F. Halouni, *J. Alloys Comp.* **381**, 21 (2004).

[10] B.C. Hauback, H. Fjellvåg, N. Sakai, *J. Solid State Chem.* **124**, 43 (1996).

[11] A.P. Ramirez, *J. Phys., Condens. Matter* **9**, 817 (1997).

[12] C.H. Chen, S.-W. Cheong, N.Y. Hwang, *J. Appl. Phys.* **81**, 4326 (1997).

[13] M.V. Zimmermann, J.P. Hill, Doon Gibbs, M. Blume, D. Casa, B. Keimer, Y. Murakami, Y. Tomioka, Y. Tokura, *Phys. Rev. Lett.* **83**, 4872 (1999).

[14] V.L. Aksenov, A.M. Balagurov, V.Yu. Pomjakushin, *Usp. Fiz. Nauk* **173**, 883 (2003).

[15] H. Kawano, R. Kajimoto, M. Kuboto, H. Yoshizawa, *Phys. Rev. B* **55**, R1479 (1996).

[16] Dipten Bhattacharya, P. Sujatha Devi, H.S. Maiti, *Phys. Rev. B* **70**, 184415 (2004).

[17] V. Dyakonov, F. Bukhanko, V. Kamenev, E. Zubov, S. Baran, T. Jaworska-Gołąb, A. Szytuła, E. Wawrzyńska, B. Penc, R. Duraj, N. Stüsser, M. Arciszewska, W. Dobrowolski, K. Dyakonov, J. Pientosa, O. Manus, A. Nabiałek, P. Aleshkevych, R. Puźniak, A. Wiśniewski, R. Żuberek, H. Szymczak, *Phys. Rev. B* **74**, 024418 (2006).

[18] V. Dyakonov, F.N. Bukhanko, V.I. Kamenev, E.E. Zubov, M. Arciszewska, W. Dobrowolski, V. Mikhaylov, R. Puźniak, A. Wiśniewski, K. Piotrowski, V. Varyukhin, H. Szymczak, A. Szytuła, R. Duraj, N. Stüsser, A. Arulraj, S. Baran, B. Penc, T. Jaworska-Gołąb, *Phys. Rev. B* **77**, 214428 (2008).

[19] J. Hemberger, M. Brando, R. Wehn, V.Yu. Ivanov, A.A. Mukhin, A.M. Balbashov, A. Loidl, *Phys. Rev. B* **69**, 064418 (2004).

[20] P.W. Anderson, H. Hasegawa, *Phys. Rev.* **100**, 675 (1955).